Supporting Information

Goldman et al. 10.1073/pnas.1312228110

SI Results

Although the active sites of BtrN and anSMEcpe show little sequence conservation (Fig. S2), a number of residues important for substrate binding are found in similar positions in 3D space, with R152, a possible proton acceptor in BtrN, being the only major exception (see Fig. 6 and *Results*). Based on mutagenesis studies, D277 was identified as a putative base in anSMEcpe (1). This residue is located on a loop in the anSMEcpe auxiliary cluster domain upstream of F278, a residue that stacks against an Aux cluster (Fig. S6). In BtrN, F188 aligns very well with D277 and stacks against its Aux cluster, which is in a slightly different position than in anSMEcpe. One residue downstream, E189 in BtrN overlays well with F278 in anSMEcpe and forms a 2.7-Å hydrogen bond with R152. Thus, E189 may be indirectly involved in deprotonation of substrate through its interaction with an arginine (*Discussion*). Two other residues in anSMEcpe, Q64 and Q98, have different orientations in the presence and absence of substrates and are proposed to play a role in substrate binding and orienting the putative base, D277 (1). In BtrN, the identities of these residues are H60 and Y90, which hydrogen bond to the C4 and C6 hydroxyl groups of the substrate, respectively (Fig. S6). These positions overlay very well in the OPEN and CLOSED BtrN structures, suggesting that their orientation does not change upon binding substrate.

Y24 was another candidate for the general base in anSMEcpe based on its position in the structure. This residue resides in the AdoMet cluster-binding loop proximal to the CX_3CX_2C motif. Although mutational studies revealed that this residue most likely does not aid in the deprotonation of intermediate (1), we find a tyrosine in a similar position in BtrN. This tyrosine, Y62, is located on a loop following the β2 strand. Whereas Y24 in anSMEcpe interacts with the adenine base of AdoMet, in BtrN, R152 wedges between AdoMet and Y62, separating it from both AdoMet and substrate binding sites (Y62 is 6.3 and 5.1 Å from AdoMet and DOIA, respectively, whereas, in anSMEcpe, Y24 is 3.9 and 3.7 Å from AdoMet and substrate) (Fig. S6). E9 is another residue in BtrN with different properties than its analogous amino acid in anSMEcpe, L7. The glutamate makes multiple hydrogen bonding interactions with the C4 and C5 hydroxyl groups of DOIA (both 2.7 Å) (Fig. S6) whereas in anSMEcpe, L7 provides a hydrophobic contact with a proline residue of the substrate peptide. Red stars in Fig. S2 mark all residues discussed in this section. Interactions provided to DOIA by the C-terminal cap are not conserved in anSMEcpe as the sites of these interactions are substituted by the anSMEcpe peptide substrate itself.

SI Materials and Methods

Cloning of the N-Terminal His_6 Tagged *btrN* Gene. The codon-optimized *btrN* gene was amplified by PCR from the plasmid pBtrNWt, which was previously derived from pET26b (2). The forward amplification primer (5′-GCC CGC GCC CGC ATA TGG ATA AAC TGT TCA GCA TGA TCG-3′) contained an NdeI restriction site (underlined) preceding 22 nt of the codon-optimized gene as well as an 11-nt GC clamp. The reverse amplification primer (5′-GGG CGGAATTCA CAG CAC GTA ATC ATA CTG TTC TTC GG-3′) contained an EcoRI restriction site that also engineered a stop codon for the gene (underlined and bold, respectively). The PCR product was isolated and digested with NdeI and EcoRI using standard procedures (3). The digested product was inserted into the pET28a expression vector that had been similarly digested. The resulting plasmid's construction was confirmed by DNA sequencing at the Pennsylvania State University core facilities and designated pNterm-BtrNWt.

Expression and Purification of *btrN* Gene-Containing Plasmids. Both the C-terminal and N-terminal His_6-tagged constructs of BtrN Wt were produced and purified as previously described (2, 4, 5). The selenomethionine (SeMet) substituted BtrN was produced by BL-21(DE3) with expression in M9 media supplemented with SeMet as previously described (6). Briefly, a 200-mL culture of LB containing 100 $\mu g \bullet mL^{-1}$ ampicillin and 50 $\mu g \bullet mL^{-1}$ kanamycin was inoculated with a single colony of BL-21 (DE3) containing pBtrNWt. This culture was grown at 37 °C for about 18 h before 40 mL was used to inoculate 4 L of M9 minimal media containing the appropriate concentration of antibiotics. The cultures were grown at 37 °C to an OD_{600nm} of 0.3 before addition of 300 mg of SeMet and 8 g of L-(+)-arabinose. The growth was continued until OD_{600nm} of 0.6, at which point 100 $mg \bullet L^{-1}$ of lysine, phenylalanine, and threonine and 50 $mg \bullet L^{-1}$ isoleucine, leucine, and valine were added to each culture. The cultures were cooled on ice for 30 min before 50 μM $FeCl_3$ was added. The cultures were placed back in an 18 °C shaker before induction of protein production with 1 mM isopropylthio-β-galactoside. The cultures were induced for 20 h at 18 °C before being harvested at 10,000 × *g* for 10 min. The cell paste was frozen and stored in liquid nitrogen until purification as previously described (2).

Crystallization. To crystallize C-terminally His_6-tagged SeMet-derivatized BtrN, a protein solution [containing 48 mg/mL C-terminally His_6-tagged SeMet BtrN, 10 mM Hepes, pH 7.5, 150 mM KCl, 10% (vol/vol) glycerol, and 5 mM DTT] was diluted in water to a final concentration of 20 mg/mL protein. AdoMet, generated enzymatically as previously described (7), was added to the solution to a final concentration of 1 mM. This mixture was allowed to incubate for 16–24 h at room temperature in an anaerobic environment (95% Ar, 5% H_2; COY Laboratory Products, Inc.). Following incubation, crystal drops using the sitting-drop vapor diffusion technique were set up by combining 1 μL of the above protein solution with 1 μL of a precipitant solution containing 13–18% (wt/vol) Jeffamine ED-2001 (pH 7.0) (Hampton Research) and 100 mM imidazole (pH 7.0). Rod-shaped crystals would grow in 3–7 d with dimensions of ~20 × 20 × 100 μm. Crystals were looped and transferred into a drop of Paratone-N (Hampton Research). This cryoprotectant was effective at shrinking the unit cell by dehydrating the crystal, leading to a more ordered lattice. After vigorous rinsing to fully exchange the mother liquor, the crystals were looped and cryocooled by direct submersion into liquid nitrogen.

To crystallize N-terminally His_6-tagged native BtrN, a protein solution (containing 138 mg/mL N-terminally His_6-tagged BtrN, 10 mM Hepes, pH 7.5, 150 mM KCl, 10% (vol/vol) glycerol, and 5 mM DTT) was diluted in water to a final concentration of either 15 or 20 mg/mL. AdoMet and DOIA, synthesized according to published procedures (7, 8), were added to a final concentration of 5 mM. This solution was incubated at room temperature for 4–8 h and then used to set up hanging-drop vapor diffusion method drops with 1 μL of the above protein solution and 1μL of a precipitant solution containing 30 mM citric acid/70 mM Bis-Tris propane (pH 7.6) and 25–31% (wt/vol) PEG 4000 (Hampton Research). Crystals would appear overnight and grow to dimensions of 50 × 50 × 300 μm in 3–7 d. For cryocooling, crystals were looped and washed through a drop of precipitant solution containing 5 mM AdoMet, 5 mM

DOIA, and 20% (vol/vol) glycerol, and then submerged in liquid nitrogen.

Data Collection and Structure Determination. An initial dataset of C-terminally His_6-tagged SeMet BtrN (Se-SAD) (Table S1) was collected at 100 K using inverse beam (1° oscillations, 30° wedges) at the selenium peak (0.9792 Å) to 2.50 Å resolution. As anomalous signal was present to better than 3 Å (phenix.xtriage), the AutoSol Wizard (9) was used to the full resolution of the dataset. Eleven heavy atom sites were found with a 0.48 figure of merit to 2.50 Å resolution. With one molecule in the asymmetric unit, these sites correspond to the 10 methionine positions in BtrN and to a peak from the BtrN auxiliary [4Fe-4S] cluster. Experimental maps were solvent flattened using RESOLVE, yielding interpretable electron density. Both [4Fe-4S] clusters and all residues (including sidechains) except for 1–3, 25–35, 116–166, and 234–250 were built into the experimental density. Using isomorphous replacement, this model was used to phase a higher resolution dataset (to 2.02 Å) collected on another SeMet BtrN crystal (Hi-res SeMet) (Table S1). Using these data, the model was completed; however, electron density for residues 28–32, 121–134, 146–161, 250, and the 19-residue C-terminal His_6 tag remained negligible. In addition, sidechain density was missing for residues 1, 26–27, 135, 164, and 248–249. This structure was refined using six TLS groups and no sigma cutoff.

A dataset of N-terminally His_6-tagged nonderivatized BtrN (AdoMet/DOIA) (Table S1) was collected at 100 K using sequential 0.5° oscillations to 1.56 Å resolution. These data were phased using molecular replacement with the Hi-res SeMet model (Phaser Z-score of 21.7 using a 4-Å resolution cutoff) (9). Electron density for missing regions of the Hi-res SeMet model is apparent using these data, including both AdoMet and DOIA substrates and the full protein chain (except for residues 161–164). The 20-residue N-terminal His_6 tag was completely disordered, as were the sidechains of residues 29, 10, 160, and 243–244. Data for all structures were collected on either beamline 24ID-E or beamline 24ID-C at the Advanced Photon Source (Argonne, IL) and processed in HKL2000 (10). All models were refined and built in PHENIX (11) and COOT (12), respectively. Composite omit maps were used to verify the final models. See Table S1 for full data processing, refinement, and validation statistics.

1. Goldman PJ, et al. (2013) X-ray structure of an AdoMet radical activase reveals an anaerobic solution for formylglycine posttranslational modification. *Proc Natl Acad Sci USA* 110(21):8519–8524.
2. Grove TL, Ahlum JH, Sharma P, Krebs C, Booker SJ (2010) A consensus mechanism for Radical SAM-dependent dehydrogenation? BtrN contains two [4Fe-4S] clusters. *Biochemistry* 49(18):3783–3785.
3. Sambrook J, Fritsch EF, Maniatis T (1989) *Molecular Cloning: A Laboratory Manual* (Cold Spring Harbor Lab Press, Plainview, New York), 2nd Ed.
4. Grove TL, Lee KH, St Clair J, Krebs C, Booker SJ (2008) In vitro characterization of AtsB, a radical SAM formylglycine-generating enzyme that contains three [4Fe-4S] clusters. *Biochemistry* 47(28):7523–7538.
5. Grove TL, et al. (2013) Further characterization of Cys-type and Ser-type anaerobic sulfatase maturating enzymes suggests a commonality in the mechanism of catalysis. *Biochemistry* 52(17):2874–2887.
6. Long F, et al. (2010) Crystal structures of the CusA efflux pump suggest methionine-mediated metal transport. *Nature* 467(7314):484–488.
7. Iwig DF, Booker SJ (2004) Insight into the polar reactivity of the onium chalcogen analogues of S-adenosyl-L-methionine. *Biochemistry* 43(42):13496–13509.
8. Yokoyama K, Ohmori D, Kudo F, Eguchi T (2008) Mechanistic study on the reaction of a radical SAM dehydrogenase BtrN by electron paramagnetic resonance spectroscopy. *Biochemistry* 47(34):8950–8960.
9. McCoy AJ, et al. (2007) Phaser crystallographic software. *J Appl Cryst* 40(Pt 4):658–674.
10. Otwinowski Z, Minor W (1997) Processing of X-ray diffraction data collected in oscillation mode. *Methods Enzymol* 276:307–326.
11. Adams PD, et al. (2010) PHENIX: A comprehensive Python-based system for macromolecular structure solution. *Acta Crystallogr D Biol Crystallogr* 66(Pt 2):213–221.
12. Emsley P, Cowtan K (2004) Coot: Model-building tools for molecular graphics. *Acta Crystallogr D Biol Crystallogr* 60(Pt 12 Pt 1):2126–2132.

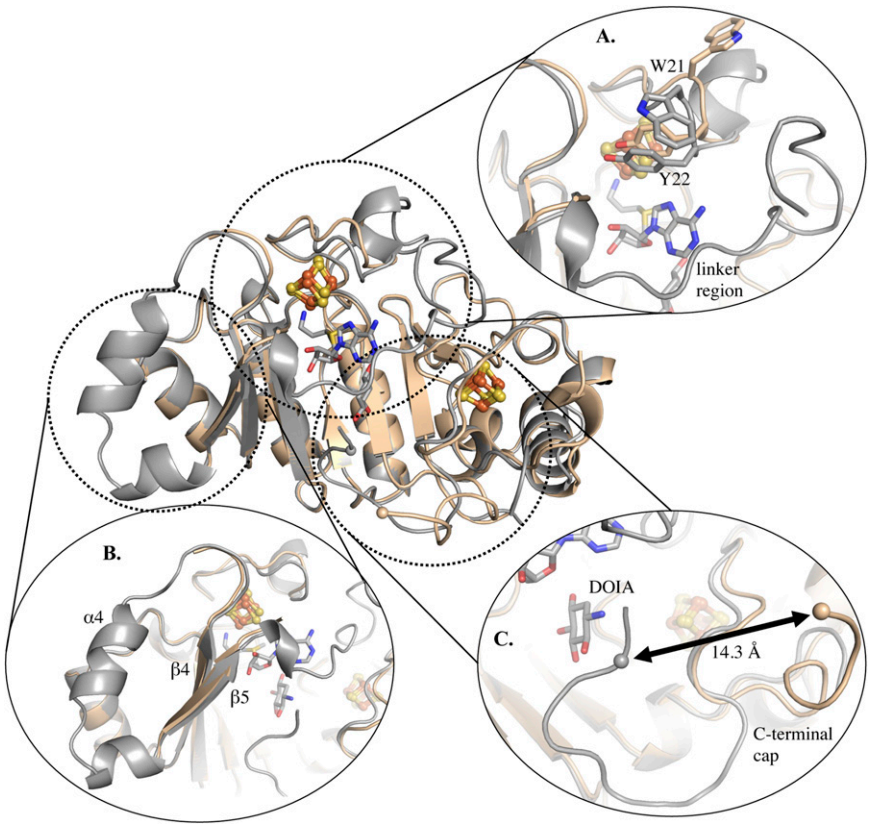

Fig. S1. OPEN (tan) and CLOSED (gray) conformations of BtrN (rmsd 0.4 Å). AdoMet and DOIA (shown in sticks) are bound to the CLOSED conformation. Both models contain two [4Fe-4S] clusters. (*Inset A*) Slight changes in the positioning of the AdoMet cluster binding loop are due to the large difference in orientation of W21. Additionally, a linker region that bridges the AdoMet and Aux cluster domains (see *Results* for domain definitions) and provides contacts to the adenine of AdoMet is disordered in the OPEN structure (after the linker region, three residues are disordered in the CLOSED structure). (*Inset B*) Although the β4 and β5 strands are superimposable in the two structures, α4 is disordered in the OPEN structure and not included in the model. (*Inset C*) The C-terminal cap in the OPEN structure leaves the DOIA binding site exposed whereas, in the CLOSED conformation, this region makes many contacts to the substrate (Fig. 2). The arrow indicates the position of the V249 Cα in the OPEN and CLOSED structures (residue 250 is modeled only in the CLOSED structure).

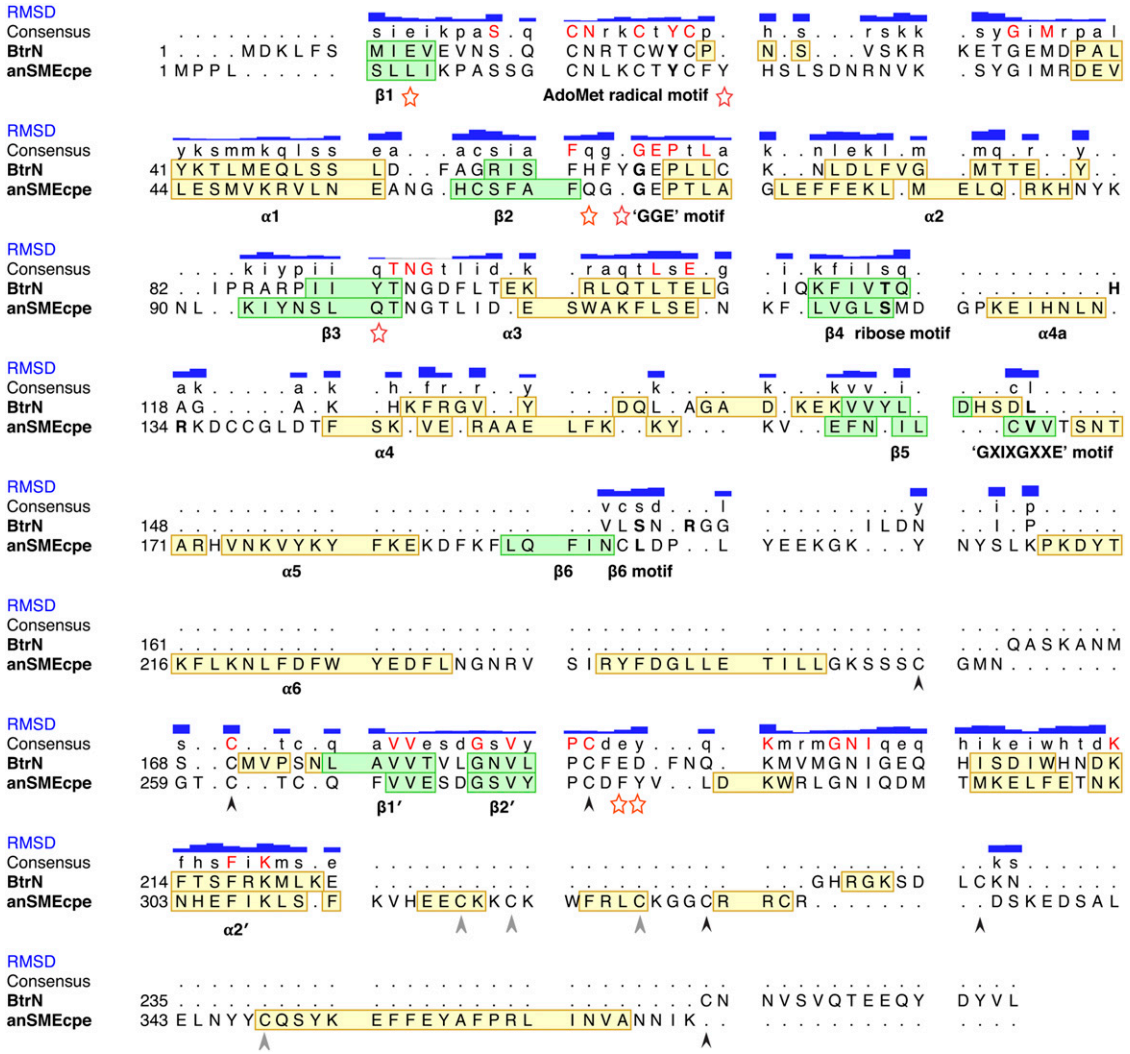

Fig. S2. Structure-based sequence alignment of BtrN and anSMEcpe. Secondary structure assignments are colored green for β-strands and yellow for α-helices. The AdoMet fold (residue 1–150 in BtrN and 1–234 in anSMEcpe) and the twitch domains, including β1′, β2′, and α2′ (residues 169–235 in BtrN and 255–311 in anSMEcpe) align well. The rmsd histogram (blue) denotes Cα distances between aligned residues and ranges from 0.05 Å (thinnest bar) to 3.9 Å (thickest bar); overall rmsd of 185 aligned residues is 2.02 Å. Strands, helices, and AdoMet radical motifs are labeled beneath the alignment (note that the GGE and GXIXGXXE motifs were named for the sequences found in BioB) (1). Residues that contact AdoMet are in bold, and red stars denote substrate binding residues discussed in *Results*. Black arrows indicate Aux cluster Fe ligating cysteines (gray arrows indicate cysteines ligating anSMEcpe's second auxiliary cluster). Alignment was generated by Chimera (2).

1. Vey JL, Drennan CL (2011) Structural insights into radical generation by the radical SAM superfamily. *Chem Rev* 111(4):2487–2506.
2. Pettersen EF, et al. (2004) UCSF Chimera—a visualization system for exploratory research and analysis. *J Comput Chem* 25(13):1605–1612.

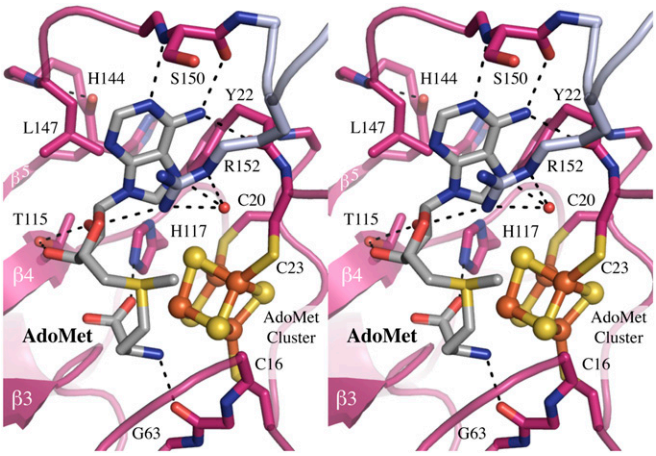

Fig. S3. AdoMet binding motifs in BtrN. Shown in stereo, BtrN (colored as in Fig. 1, rotated 90° counterclockwise from Fig. 1*D*) binds AdoMet (gray sticks) using conserved AdoMet radical structural elements, including: coordination of the amine and carboxyl groups of AdoMet by the unique iron in the AdoMet [4Fe-4S] cluster (ligated by C16, C20, and C23); hydrogen bonding of the backbone atoms of an aromatic residue to the adenine (Y22 in BtrN); the GGE motif (Y62, G63, and E64), in which backbone oxygen atoms hydrogen bond with the methionyl amine group of AdoMet; and the ribose motif (T115 and H117), in which polar residues at the end of the β4 strand hydrogen bond with the ribose hydroxyl groups (1, 2). In some cases, β4 residues, such as H117, will also hydrogen bond to the carboxyl group of AdoMet (see *Results*). The GXIXGXXE motif (L147, stabilized by a turn that includes H114), which provides hydrophobic contacts to the adenine ring, and the β6 motif (S150), which provides backbone hydrogen bonds to the adenine moiety (1, 2), are abridged in BtrN (Fig. 1*D*).

1. Vey JL, Drennan CL (2011) Structural insights into radical generation by the radical SAM superfamily. *Chem Rev* 111(4):2487–2506.
2. Dowling DP, Vey JL, Croft AK, Drennan CL (2012) Structural diversity in the AdoMet radical enzyme superfamily. *Biochim Biophys Acta* 1824(11):1178–1195.

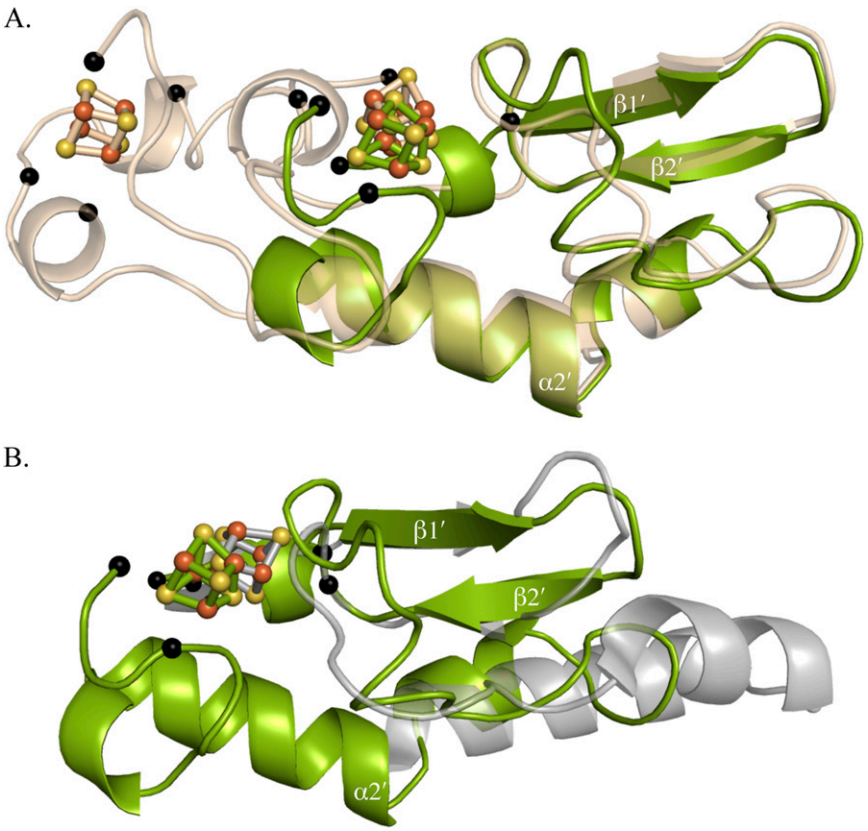

Fig. S4. Variation of the AdoMet and Auxiliary cluster fold in BtrN, compared with anSMEcpe and MoaA. Auxiliary cluster domains in BtrN (green) compared with (*A*) anSMEcpe (1) (tan), and (*B*) MoaA (2) (gray). Black spheres denote iron ligating cysteine positions. The β1′, β2′, and α2′ secondary structure elements are conserved in the three proteins (Fig. 3).

1. Goldman PJ, et al. (2013) X-ray structure of an AdoMet radical activase reveals an anaerobic solution for formylglycine posttranslational modification. *Proc Natl Acad Sci USA* 110(21):8519–8524.
2. Hänzelmann P, Schindelin H (2004) Crystal structure of the S-adenosylmethionine-dependent enzyme MoaA and its implications for molybdenum cofactor deficiency in humans. *Proc Natl Acad Sci USA* 101(35):12870–12875.

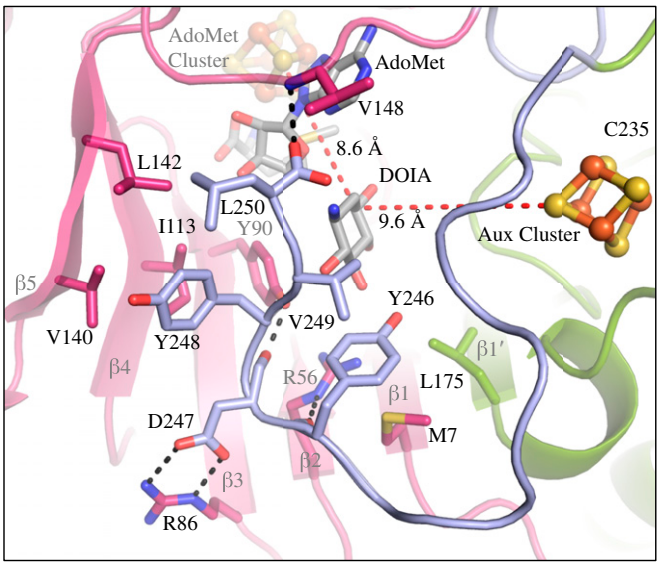

Fig. S5. Stabilization of the C-terminal cap. The active site of BtrN (colored as in Fig. 1) is sealed from solvent by the C-terminal cap, which makes numerous van der Waals and hydrogen bonding interactions with both the AdoMet domain (black dashes) and DOIA (Fig. 2*A*). The C3 position of DOIA is 8.6 Å from the AdoMet cluster and 9.6 Å from the Aux cluster (indicated by red dashes).

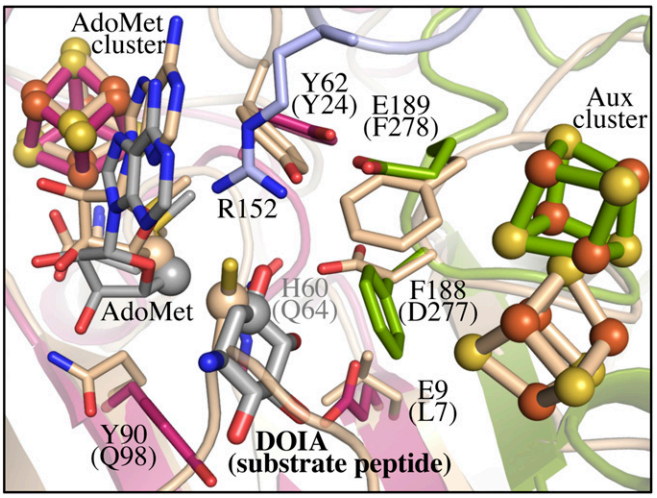

Fig. S6. Substrate binding in the AdoMet radical dehydrogenases. An overlay of the BtrN (colored as in Fig. 2) and anSMEcpe (tan) active sites. AnSMEcpe sidechains are in parentheses. The 5′ position of AdoMet and hydrogen abstraction positions of the two substrates, DOIA and substrate peptide, are in spheres.

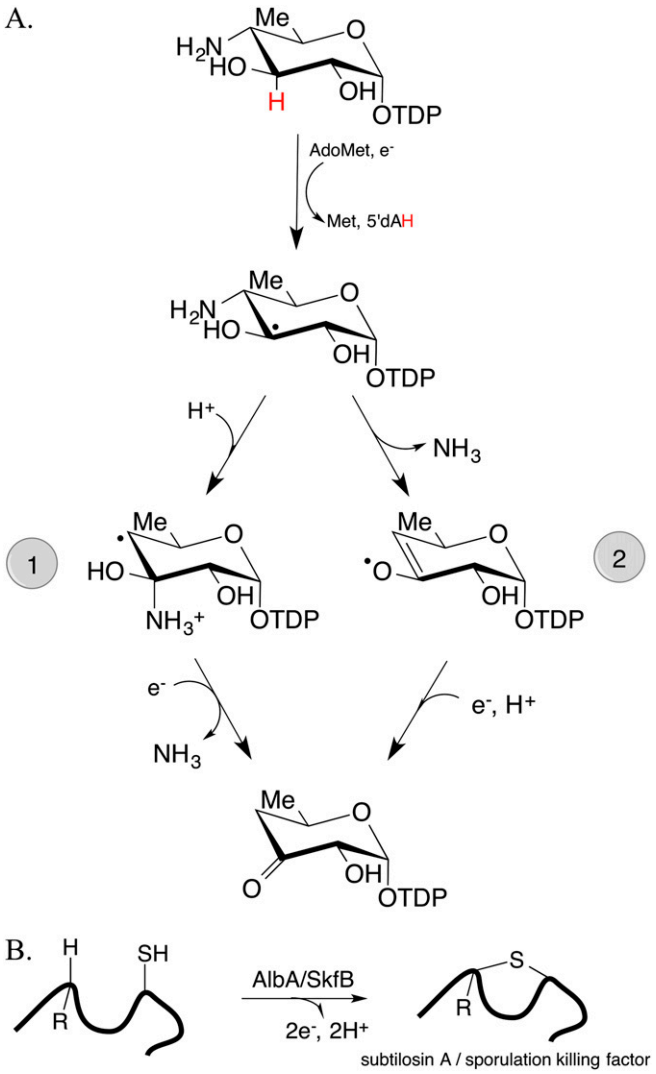

Fig. S7. Similar AdoMet radical reactions. (*A*) Two possible DesII native activity mechanisms, including (**1**) a B_{12}-like migration mechanism and (**2**) an E1cb-type mechanism. (*B*) Reactions catalyzed by the thioether bond forming enzymes, AlbA (1) and SkfB (2).

1. Flühe L, et al. (2012) The radical SAM enzyme AlbA catalyzes thioether bond formation in subtilosin A. *Nat Chem Biol* 8(4):350–357.
2. Flühe L, et al. (2013) Two [4Fe-4S] clusters containing radical SAM enzyme SkfB catalyze thioether bond formation during the maturation of the sporulation killing factor. *J Am Chem Soc* 135(3):959–962.

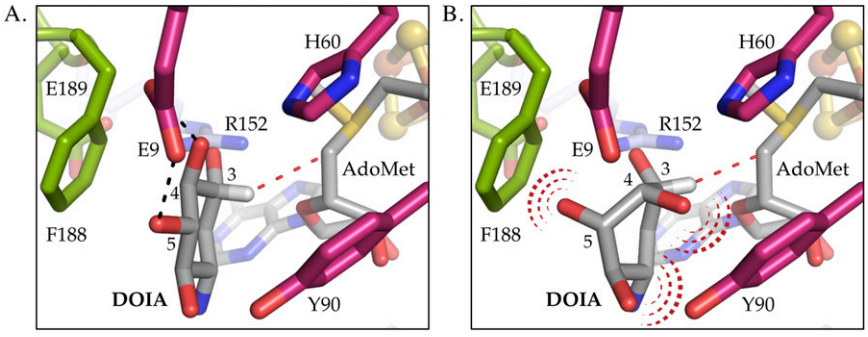

Fig. S8. Possibility of alternative DOIA conformations in BtrN. (*A*) DOIA as found in the BtrN active site (colored as in Fig. 2; C3, C4, and C5 positions labeled). Hydrogen bonds between the E9 and the C3-OH and C4-OH of BtrN (both 2.7 Å) are shown in black dashes. The C3-hydrogen is modeled in sticks (white) and the distance between it and the 5′ carbon of AdoMet is indicated by red dashes. (*B*) DOIA with a partial boat pucker is modeled into the DOIA active site. The C3 positions of both DOIA molecules are equivalent. Hydrogen bonding to E9 is no longer observed, and clashing interactions between F188 and the C5-OH and between Y90 and the C4-OH positions are now present.

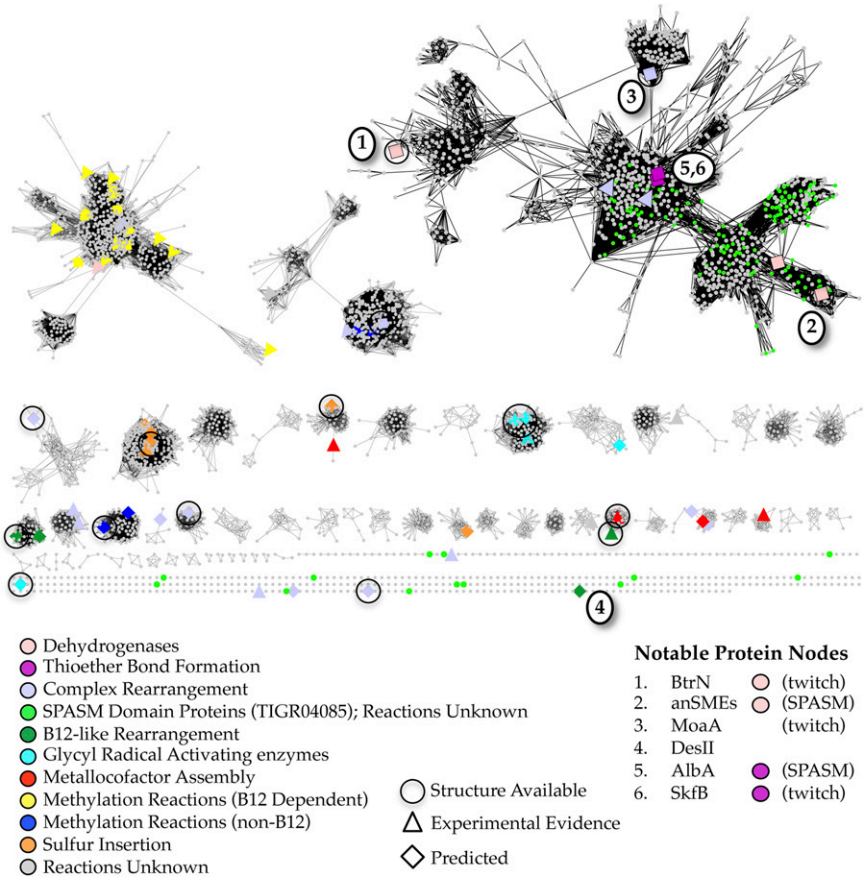

Fig. S9. The AdoMet radical superfamily. A modification of the Enzyme Function Initiative's Radical SAM Superfamily Workshop materials (http://enzymefunction.org/resources/workshops). The entire superfamily (nodes are enzymes with 40% sequence identity) is shown using a threshold cutoff of an *E*-Value of 1×10^{-22}. The figure was generated using Cytoscape (1).

1. Smoot ME, Ono K, Ruscheinski J, Wang PL, Ideker T (2011) Cytoscape 2.8: New features for data integration and network visualization. *Bioinformatics* 27(3):431–432.

Table S1. Data processing and refinement statistics for BtrN

Dataset	Se-SAD SeMet (C-term His_6)*	Hi-res SeMet (C-term His_6)*	AdoMet/DOIA (N-term His_6)
Beamline	24ID-E	24ID-C	24ID-C
Data Processing			
Wavelength, Å	0.9792	0.9795	0.9795
Space group	*C*2	*C*2	$P2_12_12_1$
Cell dimensions			
a, b, c, Å	99.6, 42.1, 50.9	99.4, 42.1, 50.9	44.6, 55.2, 116.9
β, °	104.9	105.4	
Resolution, Å†	50–2.50 (2.59–2.50)	50–2.02 (2.09–2.02)	100–1.56 (1.62–1.56)
R_{sym}, %†	12.4 (37.9)	8.7 (42.9)	11.6 (46.4)
$\langle I/\sigma(I) \rangle$ †	21.5 (4.8)	20.6 (3.0)	10.7 (2.0)
Completeness, %†	99.9 (99.1)	97.1 (74.0)	95.7 (76.0)
Redundancy†	7.6 (5.3)	5.6 (4.2)	3.9 (2.6)
Total reflections	105,617	143,572	158,698
Refinement			
Resolution, Å		38.5–2.02	58.4–1.56
Reflections		13,349	41,942
R_{work}/R_{free}		17.1/21.9	16.4/18.3
No. of nonhydrogen atoms			
Protein		1,703	1,952
[4Fe4S]/AdoMet/DOIA		16/—/—	16/27/11
Solvent		74	293
Average B-factors, $Å^2$			
Protein		38.9	20.2
[4Fe4S]/AdoMet/DOIA		29.1/—/—	19.1/19.7/17.6
Solvent		44.9	33.5
rmsd			
Bond lengths, Å		0.007	0.008
Bond angles, °		1.13	1.23
Ramachandran statistics‡		88.3%, 11.7%, 0%, 0 residues	90%, 9.6%, 0.5%, 0 residues

*Data were scaled anomalously.
†Highest resolution shell is shown in parentheses.
‡Values reported correspond to the number of residues in the most favored, additionally allowed, generously allowed, and disallowed regions, respectively.